



Molecular Crystals and Liquid Crystals Incorporating Nonlinear Optics

Publication details, including instructions for authors and
subscription information:

<http://www.tandfonline.com/loi/gmcl17>

Quadratic Hyperpolarizabilities of Some Organometallic Compounds

L-T. Cheng^a, W. Tam^a, G. R. Meredith^a & S. R. Marder^b

^a Central Research and Development Department, E. I. Du Pont
De Nemours & Co., Inc., Experimental Station, P.O. Box 80356,
Wilmington, Delaware, 19880-0356

^b Jet Propulsion Laboratory, California Institute of Technology,
4800 Oak Grove Drive, Pasadena, CA, 91109

Version of record first published: 22 Sep 2006.

To cite this article: L-T. Cheng, W. Tam, G. R. Meredith & S. R. Marder (1990): Quadratic Hyperpolarizabilities of Some Organometallic Compounds, *Molecular Crystals and Liquid Crystals Incorporating Nonlinear Optics*, 189:1, 137-153

To link to this article: <http://dx.doi.org/10.1080/00268949008037228>

PLEASE SCROLL DOWN FOR ARTICLE

Full terms and conditions of use: <http://www.tandfonline.com/page/terms-and-conditions>

This article may be used for research, teaching, and private study purposes. Any substantial or systematic reproduction, redistribution, reselling, loan, sub-licensing, systematic supply, or distribution in any form to anyone is expressly forbidden.

The publisher does not give any warranty express or implied or make any representation that the contents will be complete or accurate or up to date. The accuracy of any instructions, formulae, and drug doses should be independently verified with primary sources. The publisher shall not be liable for any loss, actions, claims, proceedings, demand, or costs or damages whatsoever or howsoever caused arising directly or indirectly in connection with or arising out of the use of this material.

Quadratic Hyperpolarizabilities of Some Organometallic Compounds

L.-T. CHENG, W. TAM and G. R. MEREDITH

*Central Research and Development Department, E. I. Du Pont De Nemours & Co., Inc.,
Experimental Station, P.O. Box 80356, Wilmington, Delaware 19880-0356*

and

S. R. MARDER

*Jet Propulsion Laboratory, California Institute of Technology, 4800 Oak Grove Drive, Pasadena, CA
91109*

The nonresonant quadratic molecular hyperpolarizabilities of several classes of organometallic aromatic compounds were studied with DC electric-field-induced second-harmonic generation (EFISH) experiments using fundamental radiation at 1.91 μm . Our goal is to survey and assess various strategies by which electron densities from metal centers can be exploited for quadratic nonlinear optics. Relying on optimized experimental techniques, systematic studies on structure-property relations concerning metal centers, bonding patterns, conjugations, and effects of ligands were conducted. Results on some arene metal carbonyl π -complexes, metal carbonyl pyridine derivatives, square-planar metal aromatics, and metallocene derivatives are included.

INTRODUCTION

Owing to the molecular nature of organic solids, questions concerning their bulk properties, such as the technologically important nonlinear optical properties, can often be addressed at the molecular level. Early realizations of large nonlinear optical polarizabilities in many molecules, prospects of optimization through molecular engineering, possibilities in developing non-crystalline bulk structures, and the potential ease of fabrications have all been motivating factors for much research activities on nonlinear optical organic materials worldwide. Despite their diversity in structures and compositions, as well as being congenial to all the considerations just mentioned, interest in organometallic compounds for nonlinear optics has been quite limited. Initial efforts^{1–7} to evaluate the potential of organometallic compounds for quadratic nonlinear optics have been restricted to using Kurtz second-harmonic generation test on powdered material. Results obtained from powder

testing are almost entirely determined by crystallographic, linear optics (*i.e.* birefringence), and dispersive factors and carry limited information on the molecular hyperpolarizabilities of organometallic molecules. Since molecular structure modification is often accompanied by crystallographic changes, powder testing cannot be used to probe structure-property relations.

Solution-phase DC electric-field-induced second-harmonic (EFISH) generation⁸ is a more appropriate method for hyperpolarizability studies. It allows extraction of a vectorial projection (β) of the hyperpolarizability tensor along the molecular dipole (μ) direction. When experiments are carried out with radiation of sufficiently long wavelength, EFISH provides direct information on the intrinsic nonlinearity of a molecule. However, there remain important limitations which should be mentioned. First, because of the rich coordination patterns and ligand structures of organometallic compounds, interpretation of EFISH results may not be possible if the molecule lacks a clear charge-transfer (CT) axis. Other tensorial components only partially active in EFISH may also be important in determining bulk properties for such compounds. Second, since the EFISH response is comprised of a rotational dipolar part which is due to the $\mu\beta$ product and an intrinsic deformational part which is due to the molecular 2nd hyperpolarizability (γ), the electronic γ contribution to EFISH signal may be significant as a result of the large polarizability of metallic composition. An estimate of this electronic contribution can be obtained from third-harmonic generation experiments only when material absorption permits. Last, the requirement of a high DC electric field precludes studies of charged organometallic pieces, many of which offer interesting structural possibilities.

A logical approach to finding quadratically nonlinear organometallic molecules is to adopt the successful strategies used in organic materials where large asymmetric polarizability is achieved by biasing the highly polarizable π electrons of a conjugated structure with donor and acceptor groups. For organics, structure-property trends concerning donor-acceptor strengths and the effectiveness of different conjugated backbones have been topics of many studies.⁹ Our recent efforts have provided an extensive set of internally consistent results on many of the important molecular classes.¹⁰ With organometallic compounds, new molecular building blocks, such as a diversity of transition metal elements at various oxidation states, filled and vacant *d* orbitals, and new bonding geometries and coordination patterns, create new possibilities for the engineering of asymmetric polarizability. In the present contribution, nonresonant EFISH measurements will be used to examine different structural approaches where a metal center can serve as either electron donor or acceptor across simple aromatic conjugations. The importance of ligand environment, metal oxidation states, and bonding patterns will be illustrated with systematic structural variations. The overall effectiveness of the organometallic approach will be contrasted with structurally similar organics.

EXPERIMENTAL

To extract the molecular hyperpolarizability β , a lengthy set of physical and optical measurements needs to be carried out. These include, on a series of solutions with

graded concentrations, measurements of density, refractive index at several wavelengths, solution capacitance, THG, and EFISH amplitudes as well as their coherence lengths for harmonic generations. These measurements respectively determine the specific volume of a solute molecule in solution, solution dispersion, solution dielectric properties, and the THG and EFISH nonlinear susceptibilities for each solution. The details of our experimental methodology and data analysis have been given elsewhere.^{10,11} We briefly describe a few key features of our experiments in this section.

The experimental setup consists of a 20 Hz Nd:YAG laser with 10 ns pulses of 0.4 J in energy. The 1.06 μm output pumps a hydrogen Raman shifter, providing up to 120 mW of Stokes-shifted radiation at 1.91 μm . This radiation serves as the fundamental frequency for both the EFISH and THG experiments, with the harmonic wavelengths at 954 nm and 636 nm respectively. For most lightly colored compounds with absorption edge at wavelengths below 500 nm, the measurement can be considered as nondispersively enhanced. THG and EFISH experiments are carried out with an unconventional technique in which the harmonic amplitudes and coherence lengths are measured separately. The laser beam is divided three ways; an intensity normalization reference branch, a coherence length measurement branch, and a harmonic amplitude measurement branch. The second and third harmonic signals from all three branches are separated with dichroic mirrors, detected with photomultiplier tubes, and collected through gated integrators.

For the determination of harmonic amplitudes, we adopted a tight focusing geometry with which the focal region of the laser beam is placed at the window-liquid interface of a "single interface" sample cell. The sample cell is equipped with a thick (2 cm) front optical window and two adjacent liquid chambers (3 cm path length) holding a reference liquid and a sample solution for comparative measurement. Electrodes are fabricated at the front window-liquid interface so that both THG and EFISH measurements can be carried out concurrently. The coherence lengths for the harmonic generations are determined with a wedged liquid cell consisting of two crystalline quartz windows, which generate sufficient second and third harmonic radiations for easy measurement. Our goal is to eliminate possible environmental contributions, which are known to be important in THG and, to a lesser extent, EFISH measurements¹²; and to increase the measurement precision by eliminating the necessity of simultaneously extracting several parameters from data fitting as is the case for the conventional Maker's fringe or wedge techniques. All experimental procedures and data acquisition scheme have been optimized to allow efficient and accurate measurements.

Figure 1 shows typical EFISH/THG amplitude (top) and dispersion (bottom) data. The amplitude data show the EFISH (\circ) and THG (\diamond) signals for an organic solution in the left chamber and for toluene in the right chamber. Clearly, the signal level (abscissa) is independent of the cell position (coordinate within each chamber, demonstrating the lack of interference arising from harmonic generations at other interfaces. The solid lines are calculated signal averages. The ratio of the harmonic intensities generated in the two chambers can be precisely determined. The dispersion data show the oscillatory periods from which coherence lengths can be extracted knowing the wedge angle of the liquid cell. The SHG coherence length

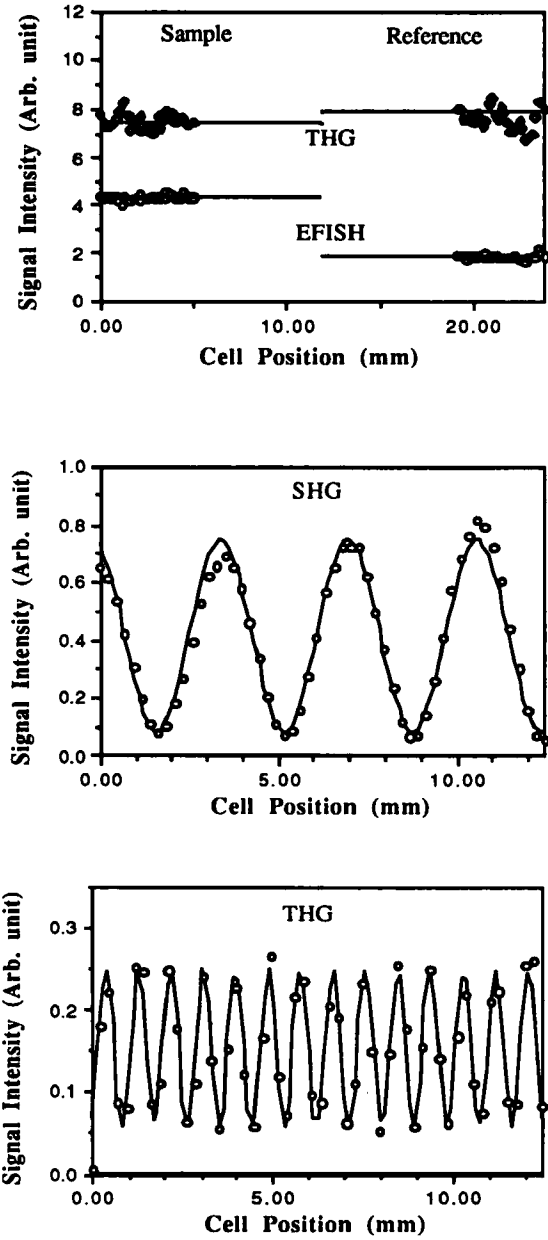


FIGURE 1 EFISH/THG amplitude (top) and dispersion (bottom) data.

is much longer than that of THG as expected. The nonzero background is a result of the focusing and finite spot size of the laser beam. The gradual rise in signal is a result of a slight wedge on one of the quartz windows. Solid lines are least square fits to determine the periods. With the known THG and EFISH nonlinearities and coherence lengths of the window material and the reference liquid (BK7-grade A glass: $\chi^{(3)}_{\text{THG}} = 4.7 \times 10^{-14}$ esu, $l_{\text{THG}} = 16.7 \mu\text{m}$, $\chi^{(3)}_{\text{EFISH}} = 3.5 \times 10^{-14}$ esu, and $l_{\text{EFISH}} = 38.8 \mu\text{m}$; toluene: $\chi^{(3)}_{\text{THG}} = 9.9 \times 10^{-14}$ esu, $l_{\text{THG}} = 18.3 \mu\text{m}$, $\chi^{(3)}_{\text{EFISH}} = 9.1 \times 10^{-14}$ esu, and $l_{\text{EFISH}} = 73.5 \mu\text{m}$),¹³ as well as the coherence lengths of the sample solution, the solution nonlinear susceptibilities can be computed.

With the measured solution properties, following the full Onsager local field model¹⁴ for both static and optical fields and taking the infinite dilution limit¹⁵ for all concentration dependent quantities, the relevant molecular properties including the dipole moment, μ , the low frequency linear polarizability, α , the hyperpolarizability, β , and the second hyperpolarizability, γ , can be calculated. The effective refractive indexes for the solute molecule in solution, as required by the Onsager model, are deduced from the solute specific volumes and high frequency polarizabilities. The vectorial component, β , of the molecular hyperpolarizability tensor along the dipole moment is calculated according to $\gamma^{\text{EFISH}} = \gamma^e + \gamma^v + \mu\beta/5kT$ where $\gamma^e + \gamma^v$, denoting a purely electronic and a hybrid vibrational contributions, is scaled with γ^{THG} . Where optical absorptions do not permit THG measurements, the electronic and vibrational contribution is taken to be 10% which is a typical value found for the more quadratically nonlinear molecules.

RESULTS AND DISCUSSION

Organometallic aromatic compounds offer several topics of interest in hyperpolarizability studies. From a structural point of view, metal arene π -complexes, where the metal center binds with all or part of the arene π electrons from one side of the arene symmetry plane, represent bonding patterns that are not found in organics. For metal pyridine complexes, coordination is achieved through the nitrogen lone pair, bearing resemblance to substituted organic aromatics. In the case of square-planar metal benzenes, the metal-carbon bond is known to be covalent in nature, providing direct organometallic analogues to the organic substituted benzenes. The sandwiched metal coordination of metallocene derivatives offer yet greater diversity in structure.

From the point of view of engineering quadratically nonlinear molecules, the generic donor-conjugation-acceptor structure which provides for high β in organic molecules can be replicated with donor or acceptor substituted aromatic ligands. The metal-carbon π -bond in arene π -complexes is a result of overlaps between metal d orbitals (d_{xz} and d_{yz}) and arene π orbitals (e_{1g} for benzene), with the metal center acting as a π -acceptor (see Figure 2). The arene ligand thus functions as both a conjugation and a π -donor. The effectiveness of interaction between arene substituents and the metal center is unclear for such a bonding arrangement. For metal pyridine complexes, the metal-nitrogen bond is largely σ in character with

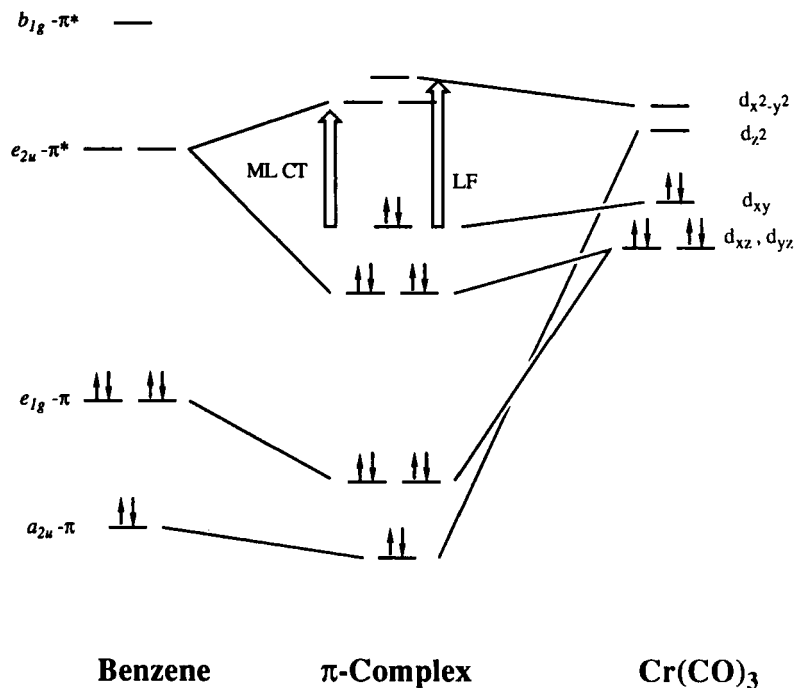


FIGURE 2 Schematic MO diagram for benzene chromium tricarbonyl π -complex.

the nitrogen lone pair flowing into the metal d orbital (d_{zz}) (see Figure 3). Coupling between 4-position substituent and the metal center should be quite effective since d - π mixing is geometrically favored. The analogy with organics is most clear with square-planar metal benzenes where the metal center is bonded covalently with a ring carbon. With metallocene derivatives, the role of the cyclopentadienyl anion may be complicated because of its formal charge which may serve as an effective donor.

Questions concerning the electronic affinities of different metal centers and how they can be influenced by their ligand environments as well as bonding geometries can also be examined. From energy consideration, metal center with d orbitals of low quantum number are expected to mix better with the π electrons of arene ligands. For metal carbonyl clusters, the strong π -accepting ability of the carbonyl ligands should enhance the status of the metal center as a π -acceptor towards the arene ligand in the ground state. Electron rich ligands such as triethylphosphine and halides should have an influence on the donating strength of a metal center. The well known trans-effect seen in chemistry involving square-planar organometallics should also be observed in hyperpolarizability studies. The redox potential of a metallocene moiety can be manipulated by different metal center and cyclopentadienyl substituents. Variation in hyperpolarizability and redox potential is expected to show correlation. In what follows, we present measurement results on the different classes of organometallic aromatic compounds just mentioned. Since our approach is empirical, we rely on chemical concepts to understand the observed

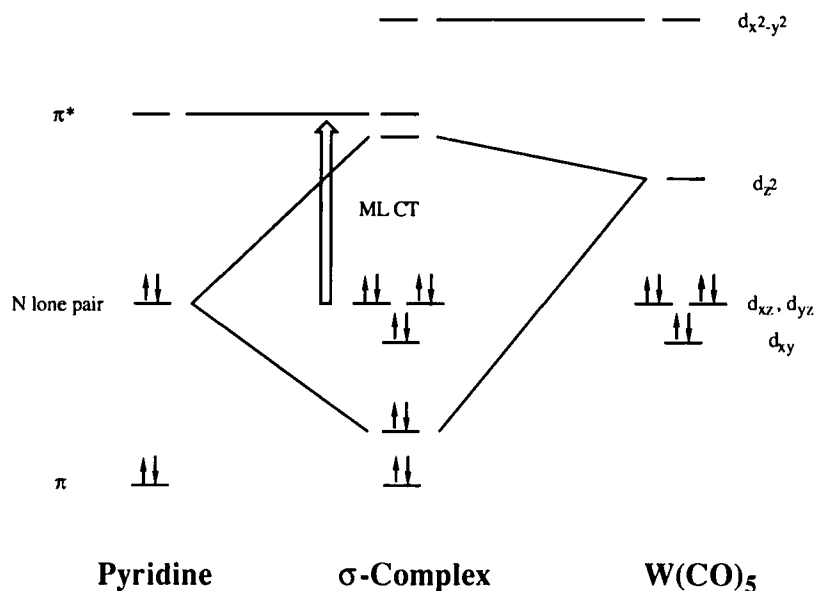


FIGURE 3 Schematic MO diagram of tungsten pentacarbonyl pyridine.

trends. Simple molecular orbital (MO) arguments and available spectroscopic evidence will be used to discuss the possible origin of nonlinearities in these structural classes. Comparison with results obtained on organics of relevant structures will be made where possible.

1. Arene metal carbonyl complexes:

Table I presents molecular parameters deduced from our solution measurements for two series of compounds: chromium tricarbonyl benzene π -complexes (π -CTCB) and tungsten pentacarbonyl pyridines (σ -TPCP) σ -complexes. Values for organics of comparable structures are also included. All quantities are given in electrostatic units as is the case throughout this paper. The peak wavelength (λ_{CT}) of the low energy and presumably charge-transfer absorption band is determined in *p*-dioxane. Error bars estimate the experimental precision of our measurements but do not include uncertainty inherent in absolute calibrations, local field, and other theoretical models involved. For both series, we have investigated the consequence of donor/acceptor substitution on the benzene or the 4-position of the pyridine ligands. Several structure-property trends are evident from the measurement results. (1) The dipole moments of both series are found to increase with the donating strength of aromatic substituents. Acceptor substituted species, **1.5** and **1.11**, have the lowest dipole moments. (2) The λ_{CT} of a well resolved peak bathochromically shifts with electron donating and accepting substituents for the π -CTCB series. The low energy spectra of the σ -TPCP series are complicated by other spectral features. (3) The signs of β are found to be invariably negative. The magnitudes of β decrease with donor strength for both series but increase sharply with acceptor substitution only

TABLE I
Results on arene metal carbonyl complexes

Compound	X	solvent	λ_{CT} (nm)	μ 10^{-18} (esu) \pm 0.1	α 10^{-23} (esu)	β 10^{-30} (esu) \pm 10%	γ 10^{-36} (esu)
Anisole		Neat	275	1.4	1.4	<0.2	5
Aniline		Neat	284	1.5	1.3	0.55	5
N,N-Dimethylaniline		Neat	293	1.6	1.7	1.1	8
Benzaldehyde		Neat	320	2.8	1.3	0.8	5
1.1	H	Toluene	310	4.4	2.3	-0.8	2
1.2	OMe	Toluene	310	4.7	2.7	-0.9	3
1.3	NH ₂	p-Diox	313	5.5	2.7	-0.6	12
1.4	NMe ₂	Toluene	318	5.5	2.9	-0.4	10
1.5	COOMe	Toluene	318	4.0	2.9	-0.7	6
1.6 trans-Phenylvinyl		p-Diox	410	4.0	4.0	-2.2	21

Compound	X	solvent	λ_{CT} (nm)	μ 10^{-18} (esu)	α 10^{-23} (esu)	β 10^{-30} (esu)	γ 10^{-36} (esu)
Pyridine		Neat	256	2.3	1.0	0.3	4
4-Acetylpyridine		CHCl ₃	276	2.7	1.5	<0.2	5
4-Aminopyridine		CHCl ₃	260	4.3	1.3	1.2	4
1.7	H	Toluene	332	6.0	3.3	-4.4	8
1.8	Phenyl	CHCl ₃	330-340	6.0	4.6	-4.5	12
1.9	Butyl	p-Diox	328	7.3	4.2	-3.4	15
1.10	NH ₂	DMSO	290	8(\pm 1)	3.5	-2.1(\pm .3)	15
1.11	COMe	CHCl ₃	420-440	4.5	4.0	-9.3	14
1.12	COH	CHCl ₃	420-440	4.6	3.7	-12	---

for the σ -TPCP series. The σ -complexes are found to be much more nonlinear and their properties highly sensitive to the 4-pyridine substituents.

As noted earlier, proper interpretation of EFISH results requires knowledge on the ground-state dipole moment. The bonding in π -CTCB compounds is comprised of electron donation from the ring to the metal center via d - π interaction, σ electron donation from the carbonyl groups, and strong back-donation from the metal to the carbonyl π orbitals. In fact, the carbonyl groups are such effective π -acceptors that despite the charge flow from the ring, the metal center is positively charged, as indicated by semiempirical MO calculations.¹⁶ Excess electron densities were found to reside at the carbonyl oxygen atoms. Thus, the ground state dipole moment is a consequence of a net CT from the ring to the metal carbonyl cluster and aligns along the molecular three-fold axis for the parent compound (1.1). For the substituted species, the dipole moment (and β) due to the ring substituent is presumably directed perpendicular to the ring-metal axis. Time averaged three-fold symmetry is preserved by a relatively free rotation about this axis. The extent of CT should be enhanced by electron donating substituents and restricted by electron with-

drawing groups on the ring. Such expectation is largely borne out by our dipole moment results (μ : $1.5 < 1.1 < 1.2 < 1.3$; $1.11 < 1.7 < 1.9 < 1.10$). However, as shown by MO calculation on the amino derivative,¹⁶ perturbation by the benzene substituent is quite weak for π -complexes.

For the σ -TPCP series, a square-pyramidal (C_{2v}) structure is known for the parent compound (1.7). The nitrogen lone pair donates in the empty d_{zz} of tungsten, forming a σ -linkage. Efficient overlap of the pyridine π orbitals with the d_{xz} or d_{yz} orbitals also allows π donation toward the metal center which acts as a potent ground state π -acceptor as a result of the pentacarbonyl ligands. It is therefore reasonable to expect that the ground-state dipole moments of the σ -TPCP derivatives are directed along the molecular two-folded axis with excess charge on the carbonyl oxygen atoms. The higher dipole moment of this series can be understood as the vectorial sum of contributions from the pyridine fragment and the metal cluster. The pyridine contribution is clearly significant when properties of pyridine and 4-pyridine derivatives are examined (see Table I). The sensitivity toward 4-position substituents is a consequence of several factors including this additive effect, the strength of the pentacarbonyl tungsten acceptor, and the importance of d - π overlaps involving the conjugated *para* position. Low solubilities as a result of the large increase in dipole moment with *para* donor substituents prevented measurements in low polarity solvents, thus introducing uncertainty from differing solvent interactions.

In order to speculate on the origin of quadratic hyperpolarizabilities in these two classes of compounds, the charge-transfer properties of their excited states must be examined. The UV-VIS absorption spectra of metallocarbonyl arene complexes are known to be dominated by metal to ligand charge-transfer (MLCT) excitations¹⁷ (see Figures 2 and 3). In particular the prominent spectral feature of benzene chromium tricarbonyl at about 310 nm has been assigned¹⁶ as a MLCT excitation in which charge densities flow from a MO of largely chromium d character to a MO of largely benzene π^* character. Similarly, d - π^* transition appears as a poorly resolved shoulder (332 nm) in the tungsten pentacarbonyl pyridine spectrum. These low lying excitations return electron densities from the metal center to the ring thus reducing their excited-state dipole moments from their ground-state values. Since, according to a simple two-state approximation,⁹ a reduction of dipole moment upon excitation leads to a negative sign for the hyperpolarizability, our observed negative β values provide strong indications of the importance of the MLCT excitations for the quadratic nonlinearity of these compounds.

The decreasing trend of β (magnitude) with increasing donating strength of ring substituents for both series can also be rationalized since strong donating groups should restrict the back transfer of charge in a MLCT excitation. In parallel with the dipole moment behavior, the σ -TPCP series shows much stronger dependence on *para* pyridine substitution. The expected enhancement of electron withdrawing substituent is however not observed with the methyl ester acceptor (1.5) for π -CTCB, probably because of the substantial positive contribution from the benzoester fragment (see values for benzaldehyde in Table I). In fact, the β values of substituted benzene chromium tricarbonyls are found to be quite insensitive to the electronic affinities of the substituents. This is perhaps not surprising since the

metal donor is not truly “in conjugation” with the benzene substituents. The weak bathochromic shift of the CT band in both donor and acceptor substituted π -complexes also indicates poor CT interactions. Much stronger structure-property variations, in CT band positions (290–430 nm), dipole moments (4.5–8.0 Debye), and β values (-2.1 to -12×10^{-30} esu), are found for the pyridine tungsten pentacarbonyls, reflecting the greater structural similarity of this class of compounds to donor-acceptor conjugated organics. The filled d_{xz} and d_{yz} orbitals have the proper nodal patterns (sign change across the pyridine plane) to participate in the 4-substituted pyridine π system. The substantially higher nonlinearity of this series over the π -CTCB series can be rationalized with the same considerations of the charge back transfer. (The low value of the amino derivative (**1.10**) is probably also influenced by the substantial positive contribution from the 4-aminopyridine moiety.) Their CT bands are seen to hypsochromically shift with 4-substituted donor strength and bathochromically shift with acceptor strength for a range of over 40 nm. Negative solvatochromic behaviors are also known for these compounds¹⁸ indicating a lower excite-state dipole moment, in agreement with the observed negative sign of β as interpreted via the two-state model.

The electronic properties of the metal carbonyl cluster appear to be those of an effective ground-state acceptor and excited-state donor, a characteristic not found in common organic substituents. This characteristic allows for highly nonlinear molecular structure with low ground-state dipole moment; thus favoring acentric crystal packing for bulk nonlinearity, at least in principle. However, the σ -TPCP series did not yield any appreciable bulk response according to powder testing.¹ It is instructive to note that for the more nonlinear of the two series, the magnitude of their β values are comparable to conventional nonlinear organics such as *p*-nitroaniline ($\mu = 6.2 \times 10^{-18}$ esu and $\beta = 9.2 \times 10^{-30}$ esu). With stronger accepting group such as cyano, the β value can be further enhanced.

2. Square-Planar Metal Aromatics

Table IIa shows measurement results on several square-planar platinum and palladium benzene derivatives. Since the metal-carbon bond is covalent in nature, these compounds represent an organometallic analogue to the highly nonlinear donor-acceptor para-disubstituted benzenes. Powder SHG testing revealed that this class of compounds is indeed nonlinear and show a propensity to crystallize in noncentrosymmetric forms, yielding powder-SHG signal as high as 14 times urea.⁶ Our interests in this series of compound arise from the knowledge that $-MX(PEt_3)_2$, where M = Ni, Pd, and Pt; X = I, Br, Cl, and others, are good electron donors. Their donating strengths also have marked dependence on the nature of the *trans* ligand. The inductive and resonance substituent parameters, as determined by ¹⁹F Nmr studies,¹⁹ are reproduced in Table IIb. Notice that the square-planar metal groups are both inductive and resonance donors. The inductive contribution is quite strong and is sensitive to the nature of the *trans* ligand. Spectroscopic studies²⁰ have also revealed a *cis* influence which is comparable in strength but opposite in sign to the *trans*-effect.

The extent of charge flow from the metal center to the ring through the σ -linkage

TABLE IIa
Results on square-planar metal benzenes

Compd	A	M	L	X	solvent	$\mu \cdot 10^{-18}$ (esu) ± 0.2	$\alpha \cdot 10^{-23}$ (esu)	$\beta \cdot 10^{-30}$ (esu) $\pm 15\%$	$\gamma \cdot 10^{-36}$ (esu)
2.1	CHO	Pt	PEt ₃	Br	CHCl ₃	2.5	5.8	2.1	37
2.2	NO ₃	Pd	PEt ₃	I	CHCl ₃	3.6	6.2	0.5	36
2.3	NO ₂	Pd	PPh ₃	I	CHCl ₃	5.5	1.05	1.5	50
2.4	NO ₂	Pt	PEt ₃	I	CHCl ₃	3.0	6.2	1.7	36
2.5	NO ₂	Pt	PEt ₃	Br	CHCl ₃	3.4	6.1	3.8	55

TABLE IIb
Inductive and resonance substituent parameters for *trans*-MX(PEt₃)₂ groups

<i>trans</i> -Ligand X	σ_1			σR^0		
	Ni	Pd	Pt	Ni	Pd	Pt
CH ₃	-0.50	-0.46	-0.51	-0.28	-0.24	-0.25
C ₆ H ₅	-0.42	-0.40	-0.44	-0.28	-0.24	-0.25
Br	-0.20	-0.11	-0.24	-0.32	-0.27	-0.26
I	-0.16	-0.08	-0.20	-0.32	-0.27	-0.26

is determined by the σ -donating strength of the *trans* ligand and the accepting strength of the *para* benzene substituent. *d*- π interaction also exists for *d* orbitals of proper symmetry. For a *d*⁸ square-planar complex (with the z-axis perpendicular to the ligand plane), the HOMO is largely *d*_{xy} in character (see Figure 4). Single crystal x-ray⁶ reveals that for Pt(PEt₃)₂(I)(*p*-nitrophenyl), compound 2.4, the ligand plane is oriented perpendicular to the nitrophenyl mirror plane, allowing effective *d*- π overlap between the metal *d*_{xy} orbital and the benzene π system. Such interaction is not possible if the two planes are in a parallel arrangement. Thus, para substituent should be in conjugation with the metal center and is expected to have significant effect on hyperpolarizability.

Overall, measurement results in Table IIa is in agreement with expectation based on substituent parameters. All β values are found to be positive showing the analogy with disubstituted aromatics. Platinum compounds are found to be more nonlinear than palladium compounds (2.2 vs 2.4), reflecting the substantial difference in inductive donating strength between the two metal centers (see Table IIb). The *trans* influence is also evident with the bromo ligand significantly better than iodo ligand for nonlinearity (2.5 vs 2.4). The strong *cis* influence is seen by replacing the triethylphosphine ligands with the less electron rich triphenylphosphine. Since

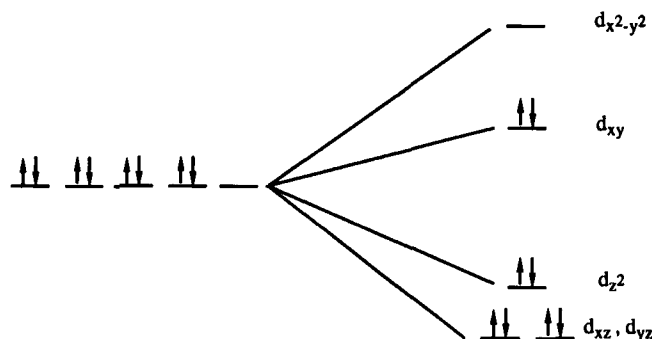


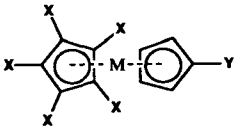
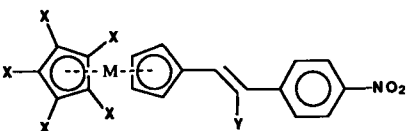
FIGURE 4 Ligand-field splitting of d orbitals for square-planar d^8 -metal complex.

the *cis* influence is opposite in sign with the *trans*-effect, a reduction in *cis* donation actually leads to a strengthening of charge-transfer for the *trans* ligands; thus resulting in significant increases in both dipole moment and hyperpolarizability (2.2 vs 2.3). The importance of the benzene acceptor is also evident. Both dipole moments and β values are found to increase with acceptor strength, giving the higher values for the nitro derivatives (2.5 > 2.1). Based on the current findings, nonlinearity optimization of this class of compound requires nickel as the metal center to maximize resonance donation, good donor such as methyl or methoxy as the *trans* ligand, poor donor for the *cis* ligands, and strong acceptor for the *para*-phenyl substituent.

3. Metallocene

Metallocene derivatives, with iron group metallocenes in particular, represent interesting and novel structural variations in the studies of molecular hyperpolarizabilities. A ferrocene derivative, *cis*-1-ferrocenyl-2-(4-nitrophenyl)ethylene (3.4), have been shown to possess rather large bulk SHG activity (62 times urea).³ Given the aromatic character of the cyclopentadienyl ring and the propensity of the metal center to undergo redox chemistry, one may speculate on the potential for effective charge-transfer when a metallocene is bonded in conjugation with an electron acceptor. However, since the metal is centrally π -bonded to two cyclopentadienyl rings (Cp), akin to the weakly nonlinear chromium tricarbonyl benzene derivatives (see Table I), and the ring aromaticity also results in a formal divalence on the metal center, the donating ability of the metallocene is potentially complicated. At the least, it will be dependent on the oxidation potential of the metal nucleus and additional substituents on both five-membered rings. To assess the effectiveness of using metallocene donors for nonlinear optics, we have characterized the hyperpolarizabilities of several metallocene derivatives and have examined various structural dependencies. Measurement results on ferrocene and ruthenocene derivatives are summarized in Table III. Compounds 3.1 and 3.2 represent the cyclopentadienyl analogues of acceptor substituted benzenes. Compounds 3.3 to 3.11 carry structural resemblance to some nitrostilbenes whose nonlinear properties have been previously studied.¹⁰ By comparing current results with those obtained for

TABLE III
Results on metallocene derivatives

Compound	M	X	Y	solvent				
					λ_{\max} (nm)	$\mu \cdot 10^{-18}$ (esu) ± 0.1	$\alpha \cdot 10^{-23}$ (esu)	$\beta \cdot 10^{-30}$ (esu) $\pm 10\%$
3.1	Fe	H	COCH ₃	p-Diox	—	3.0	2.6	0.3 \pm 0.2
3.2	Ru	Me	NO ₂	CH ₂ Cl ₂	—	5.5	3.9	0.6 \pm 0.2
Compound	M	X	Y	solvent				
					λ_{CT} (nm)	$\mu \cdot 10^{-18}$ (esu)	$\alpha \cdot 10^{-23}$ (esu)	$\beta \cdot 10^{-30}$ (esu)
3.3	Fe	H	H(<i>trans</i>)	p-Diox	356/496	4.5	3.9	31
3.4	Fe	H	H(<i>cis</i>)	p-Diox	325/480	4.0	3.8	13
3.5	Fe	Me	H	p-Diox	366/533	4.4	5.3	40
3.6	Fe	H	CN	p-Diox	348/526	5.3	4.2	21
3.7	Fe	Me	CN	p-Diox	366/560	6.0	5.6	35
3.8	Ru	H	H	p-Diox	350/390	5.3	4.2	12
3.9	Ru	Me	H	p-Diox	370/424	5.1	5.0	24
3.10	Ru	Me	CN	p-Diox	370/443	5.9	5.5	24
3.11	Fe	H	H	p-Diox	366/536	4.9	4.5	23
3.12	Fe	H	H	p-Diox	382/500	4.5	4.6	66

benzene and stilbene derivatives, the nonlinearities of the metallocene derivatives can be put into perspective. Several structural variations, including different metal centers, *cis* and *trans* conformations, extension of conjugation, symmetric electron donating substituents in the form of pentamethyl cyclopentadienyl rings (Cp^*), and ethylenic cyano as well as 2,4-dinitro substitutions, have been implemented.

Despite some quantitative details, the electronic structure and bonding interactions of ferrocene can be considered as well understood.²¹ Briefly, the chemical stability of ferrocene is partly a result of the inert gas valence of the metal center whose 8 valence electrons are joined by 5 π electrons from each of the Cp's (see Figure 5). Eight electrons reside in 4 strongly bonding orbitals which are largely π ring-orbital in character. Four electrons occupy two bonding orbitals which are largely π ring-orbital in character. Four electrons occupy two bonding orbitals which provide the key d - π interactions between the ring e_{1g} and the metal d_{xz} and d_{yz} orbitals, resulting in the sandwiched structure. The remaining six electrons fill the largely nonbonding MOs which are essentially the d_{zz} , d_{xy} , and d_{xx-yy} of the metal center. Although there remains disagreement on their relative order, d_{zz} is generally accepted as the HOMO of ferrocene. In any case, these electrons are weakly bound and are available for redox chemistry and CT interaction with ac-

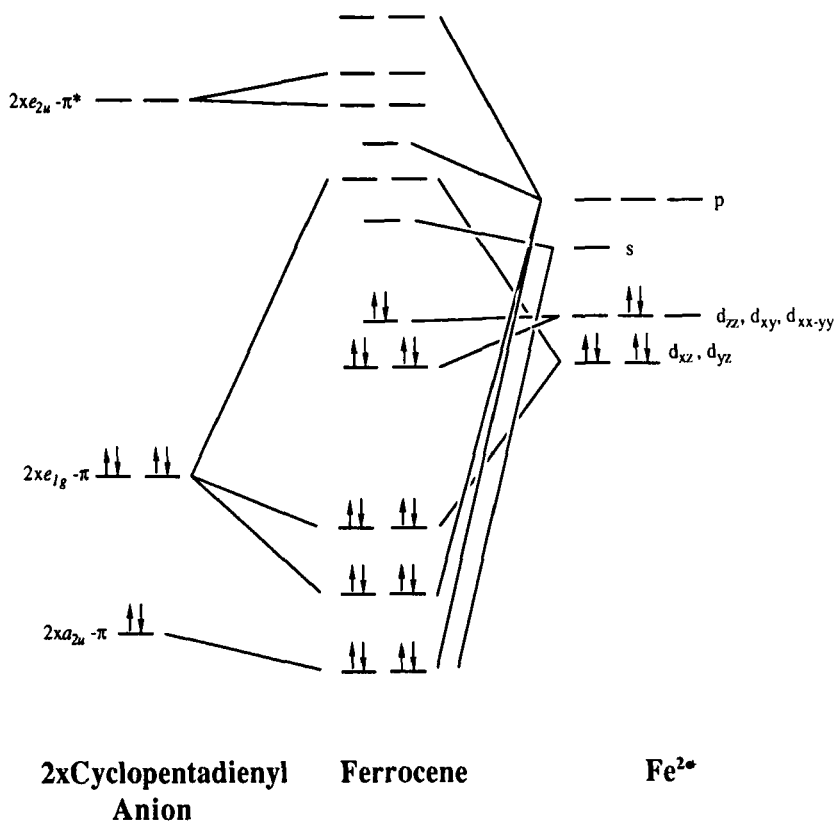


FIGURE 5 Schematic MO diagram for ferrocene.

cepting orbitals. The donated electron density for CT in an acceptor substituted analogue is therefore largely from the metal center. This is unlike the situation found in acceptor substituted benzenes where electron densities move from a filled bonding π -orbital of benzene to an empty low lying orbital of the substituent. With ruthenocene, this MO picture remains relevant. The nonbonding d orbitals may shift in energy thus affecting its redox potential and donating strength. Clearly the electron affinity of the metallocene depends strongly on the metal center and it is not valid to think of the metallocene merely as a 5-member aromatic anion with the metal center providing a full electron.

The low energy spectra of metallocenes are dominated by two equally strong bands (325 nm and 440 nm for ferrocene; 277 nm and 321 nm for ruthenocene) that are basically ligand field transitions. Both states have some ring orbitals mixed in thus is somewhat CT in the character. The higher energy state apparently is more so since it gains prominence over the other band upon acceptor substitution. This occurs to a lesser extent for the ruthenocene derivatives. Both bands bathochromically shift with acceptor substituents. Solvatochromic behavior has been observed for compounds **3.3**, **3.5**, and **3.7**. The lower lying bands are found to red shift by about 8–10 nm and the higher lying bands by somewhat less between *p*-dioxane and acetonitrile solutions. Pentamethyl, ethylenic cyano, and 2,4-dinitro substitutions all lead to large bathochromic shift of these absorption bands. Only the higher energy band of 4-nitrophenyl butadiene ferrocene (**3.12**) is significantly red-shifted. It also becomes much stronger than the lower energy band. The importance of these transitions to the observed quadratic hyperpolarizabilities awaits full assessment by theoretical investigations.

Compound **3.1** and **3.2** show somewhat larger dipole moments but substantially lower β values in comparison with their benzene analogues. The polar nature of acceptor substituted ferrocene have been noted before²² and was taken as an indication of a pronounced electron releasing capacity of the ferrocene rings. The dipole moment of the ruthenium compound (**3.2**) is particularly high given a value of only 4.0 Debye for nitrobenzene. This is likely a result of the electron releasing pentamethyl substitution which enhances the donating strength of even the opposite ring. This effect is clearly seen among all the compounds investigated (e.g. **3.3** vs **3.5** and **3.8** vs **3.9**). The ruthenocene derivatives are found to be more polar than their ferrocenyl analogues, which is somewhat surprising considering the higher oxidation potential of ruthenocene. This may be a result of the lower energy, relative to the acceptor orbital, and the greater spatial extent of the $4d$ orbitals.

The low β values for compounds **3.1** and **3.2** may be due to the poorly defined CT axes since the metal-ring bond is perpendicular to the ring substituent bond. This is somewhat analogous to the chromium tricarbonyl π -complexes examined earlier (compound **1.6** shows significant enhancement with the stilbene conjugation). Other derivatives which have a well defined charge transfer direction along the 4-nitrophenylvinyl group, show respectable nonlinearities in comparison with nitrostilbene ($\beta = 9.1 \times 10^{-30}$ esu), 4-4'-methoxynitrostilbene ($\beta = 29 \times 10^{-30}$ esu), and 4-4'-dimethylaminonitrostilbene ($\beta = 75 \times 10^{-30}$ esu). Since these compounds have long wavelength absorption bands, the measured nonlinearity is dispersively enhanced. The *cis* compound (**3.4**) is found to be less nonlinear than

the *trans* compound (3.3) as expected, considering the lower 2nd hyperpolarizability of *cis*-stilbene and the shorter conjugation length because of the bent charge-transfer pathway. Pentamethyl substitution at the opposite ring significantly enhances both the dipole moment and the nonlinearity. This agrees with the intuition that the added charge density should lower the real charge of the metal center thus enhancing the donating strength of the metal *d* electrons. The HOMO is clearly destabilized leading to a large spectral red shift. Redox potential studies also reveal a substantial decrease²³ of quarter-wave potential (vs SCE) with Cp donor substituted species. Ethylenic cyano and 2,4-dinitro substitutions lead to spectral red shifts, an increase of dipole moment, and an apparent decrease of nonlinearity. This is similar to previous observations on stilbene derivatives.¹⁰ The lowering of the EFISH β may partially be a result of an induced change in dipole direction by the strong accepting side groups, deviating from the long molecular axis. The effect on the conjugation length is dramatic with compound 3.12 exhibiting a significantly higher β value. The dipole moment shows only a modest increase. This is again in agreement with structural trends observed in stilbene derivatives. The ruthenium compounds are found to be less nonlinear than their iron counter parts. If the charge-transfer is from the metal center to the acceptor group, the higher oxidation potential²³ of ruthenocene would result in lower nonlinearity. The larger dipole moment of the ruthenium compounds remains puzzling.

CONCLUSION

The hyperpolarizabilities of several classes of organometallic aromatic compounds have been systematically investigated with off-resonant EFISH and THG measurements. Our findings concerning quadratic hyperpolarizabilities can be summarized as follows: (1) The dipole projections of the β tensors of arene tricarbonyl chromium π -complexes are found to be small and their properties are quite independent of arene substituents. These observations are attributed to poor coupling between the metal center and substituent because of the π geometry. (2) Tungsten pentacarbonyl pyridine derivatives show respectable nonlinearities and are highly sensitive to 4-position substituents. The symmetry favored addition of accepting strengths of the metal cluster and the pyridine nitrogen leads to a highly polar ground-state. Hyperpolarizabilities higher than that of *p*-nitroaniline have been observed with acceptor substituted species because of effective *d*- π interactions with substituents. (3) The β values of metal carbonyl derivatives are always negative, indicating reversal of signs for CT in the ground and excited states. This observation is consistent with simple MO pictures for these two classes of materials whose low energy excitations are metal to ligand CT in nature. (4) Square-planar platinum and palladium benzenes are moderately nonlinear, with β values comparable to methoxy substituted benzenes. The ligand environment is seen to be a decisive factor influencing hyperpolarizability. (5) Ferrocene derivatives provided the highest nonlinearity found in the present study, approaching that of 4,4'-dimethylamino nitrostilbene. The donating strengths of the metallocenes are attributed to the low binding energy of metal electrons and their effectiveness is responsive to structural modifications which also influence their redox potentials.

(6) Overall, one can conclude that the adaptation of donor-conjugation-acceptor strategies involving organometallic end groups are successful in engineering molecular hyperpolarizability, resulting in species with nonlinearities comparable to those found in organics. Interesting behaviors of CT not commonly seen in organics are observed with organometallic species. The principle disadvantage of some of the materials examined is their chemical instabilities. This shortcoming can probably be expected in other organometallics considering the nature of metal-ligand coordinations. The metallocene derivatives are however chemically quite stable.

Acknowledgments

The authors thank H. Jones, T. Hunt, and B. Tiemann for expert technical assistance. Part of the research presented in this paper was performed by the Jet Propulsion Laboratory, California Institute of Technology as part of its Center for Space Microelectronics Technology which is supported by the Strategic Defense Initiative Organization, Innovative Science and Technology Office through an agreement with National Aeronautics and Space Administration.

References

1. C. C. Frazier, M. A. Harvey, M. P. Cockerham, H. M. Hand, E. A. Chauchard and C. H. Lee, *J. Phys. Chem.*, **90**, (1986) 5703.
2. D. F. Eaton, A. G. Anderson, W. Tam and Y. Wang, *J. Am. Chem. Soc.*, **109**, (1987) 1886.
3. M. L. H. Green, S. R. Marder, M. E. Thompson, J. A. Bandy, D. Bloor, P. V. Kolinsky and R. J. Jones, *Nature*, **330**, (1987) 360.
4. J. C. Calabrese and W. Tam, *Chem. Phys. Lett.*, **133**, (1987) 244.
5. A. G. Anderson, J. C. Calabrese, W. Tam and I. D. Williams, *Chem. Phys. Lett.*, **134**, (1987) 392.
6. W. Tam and J. C. Calabrese, *Chem. Phys. Lett.*, **144**, (1988) 79.
7. S. R. Marder, J. W. Perry and W. P. Schaefer, *Science*, **245**, (1989) 626.
8. B. F. Levine and C. G. Bethea, *Appl. Phys. Lett.*, **24**, (1974) 445.
9. See for example: J. F. Nicoud and R. J. Twieg, in "Nonlinear Optical Properties of Organic Molecules and Crystals," edited by D. S. Chemla and J. Zyss. Vol. 2 Academic Press, NY (1987) 255 and reference therein.
More recently, R. A. Huijts and G. L. J. Hesselink, *Chem. Phys. Lett.*, **156**, (1989) 209; M. Barzoukas, M. Blanchard-Desce, D. Josse, J.-M. Lehn and J. Zyss, *Chem. Phys.*, **133**, (1989) 323.
10. L. T. Cheng, W. Tam, G. R. Meredith, G. Rikken and E. W. Meijer, *SPIE Proc.*, **1147**, (1989) 61.
11. G. R. Meredith, L. T. Cheng, H. Hsiung, H. A. Vanherzeele and F. C. Zumsteg, "Materials for Nonlinear and Electro-optics," edited by M. H. Lyons, The Institute of Physics (IOP Publishing), New York (1989) 139.
12. G. R. Meredith, B. Buchalter and C. Hanzlik, *J. Chem. Phys.*, **78**, (1983) 1533. G. R. Meredith, *Optics Comm.*, **39**, (1981) 89.
13. B. Buchalter and G. R. Meredith, *Appl. Optics*, **21**, (1982) 3221. S. H. Stevenson, (1988) unpublished.
14. See for example: C. J. F. Bottcher, "Theory of Electric Polarization," 2nd ed. Elsevier, NY (1973).
15. K. D. Singer and A. F. Garito, *J. Chem. Phys.*, **75**, (1981) 3572.
16. D. G. Carroll and S. P. McGlynn, *Inorg. Chem.*, **7**, (1968) 1285.
17. G. L. Geoffroy and M. S. Wrighton, "Organometallic Photochemistry," Academic: New York (1979).
18. M. S. Wrighton, H. B. Abrahamson and D. L. Morse, *J. Am. Chem. Soc.*, **98**, (1976) 4105.
20. D. P. Arnold and M. A. Bennett, *Inorg. Chem.*, **23**, (1984) 2117.
21. See for example: M. Rosenblum, "Chemistry of the Iron Group Metallocenes," Interscience, Wiley & Son: New York (1965), Chapter 2.
22. H. H. Richmond and H. Freiser, *J. Am. Chem. Soc.*, **77**, (1954) 2022.
23. T. Kuwana, D. E. Bublitz and G. L. K. Hoh, *J. Am. Chem. Soc.*, **82**, (1960) 5811.